



LAWRENCE  
LIVERMORE  
NATIONAL  
LABORATORY

# A low-permeability underground nuclear explosion containment regime: An example of gas transport by "invisible" fractures?

C. R. Carrigan, Y. Sun, S. Hunter, D. Ruddle

June 13, 2019

Nature Scientific Reports

## **Disclaimer**

---

This document was prepared as an account of work sponsored by an agency of the United States government. Neither the United States government nor Lawrence Livermore National Security, LLC, nor any of their employees makes any warranty, expressed or implied, or assumes any legal liability or responsibility for the accuracy, completeness, or usefulness of any information, apparatus, product, or process disclosed, or represents that its use would not infringe privately owned rights. Reference herein to any specific commercial product, process, or service by trade name, trademark, manufacturer, or otherwise does not necessarily constitute or imply its endorsement, recommendation, or favoring by the United States government or Lawrence Livermore National Security, LLC. The views and opinions of authors expressed herein do not necessarily state or reflect those of the United States government or Lawrence Livermore National Security, LLC, and shall not be used for advertising or product endorsement purposes.

1 **A low-permeability underground nuclear explosion**  
2 **containment regime: An example of gas transport**  
3 **by “invisible” fractures?\***  
4

5 Charles R. Carrigan<sup>1†</sup>, Yunwei Sun<sup>1</sup>, Steven L. Hunter<sup>1</sup>, David G. Ruddle<sup>1</sup>, Matthew  
6 D. Simpson<sup>1</sup>, Curtis M. Obi<sup>2</sup>, Heather E. Huckins-Gang<sup>2</sup>, Lance B. Prothro<sup>2</sup>, Mar-  
7 garet J. Townsend<sup>2</sup>  
8

9 <sup>1</sup>Lawrence Livermore National Laboratory, Livermore, California, USA

10 <sup>2</sup>Mission Support and Test Services, LLC, Las Vegas, Nevada, USA

11 Understanding the nature of gas transport from an underground nuclear explosion  
12 (UNE) is required for evaluating the ability to detect and interpret either on-site  
13 or atmospheric signatures of noble gas radionuclides resulting from the event. We  
14 performed a pressure and chemical tracer monitoring experiment at the site of an  
15 underground nuclear test that occurred in a tunnel in Nevada to evaluate the possible  
16 modes of gas transport to the surface. The site represents a very well-contained, low  
17 gas-permeability end member for past UNEs at the Nevada National Security Site.  
18 However, there is very strong evidence that gases detected at the surface during a  
19 period of low atmospheric pressure resulted from fractures of extremely small aperture  
20 that are essentially invisible. Our analyses also suggest that gases would have easily  
21 migrated to the top of the high-permeability collapse zone following the detonation  
22 minimizing the final distance required for migration along these narrow fractures  
23 to the surface. This indicates that on-site detection of gases emanating from such  
24 low-permeability sites is feasible while standoff detection of atmospheric plumes may  
25 also be possible at local distances for sufficiently high fracture densities. Finally, our  
26 results show that gas leakage into the atmosphere also occurred directly from the  
27 tunnel portal and should be monitored in future tunnel gas sampling experiments for  
28 the purpose of better understanding relative contributions to detection of radioxenon  
29 releases via both fracture network and tunnel transport.

---

\*Revised for publication in *Nature – Scientific Reports* (September 4, 2019).

†Correspondence and requests for materials should be addressed to C.R. Carrigan (e-mail address:  
carrigan1@llnl.gov).

IM release number: LLNL-JRNL-777779

30 As part of the National Nuclear Security Administration’s (NNSA) program to  
31 evaluate different signatures that are characteristic of underground nuclear explo-  
32 sions (UNEs), we have embarked on a multi-year study of two UNE containment sites  
33 having extremely different gas transport characteristics. The first phase of the study  
34 focused on the containment site resulting from the 1989 Barnwell UNE carried out  
35 within the volcanic layering of Pahute Mesa at the Nevada National Security Site  
36 (NNSS). That UNE used a vertical emplacement design having a detonation point at  
37 600 m depth and an explosive yield between 20 and 150 kilotons [1]. This “open” con-  
38 tainment regime end-member was found to have a characteristic bulk gas permeability  
39 of more than 4 Darcys ( $1 \text{ Darcy} = 1.0 \times 10^{-12} \text{ m}^2$ ) as shown in Table 1 of [2].

40 More recently the Barnwell end-member has been used to simulate atmospheric  
41 signatures resulting from the seepage of gases from the detonation cavity or chimney  
42 to the surface and into the atmosphere [3]. Using coupled simulations of subsurface  
43 and atmospheric transport, it was found that current levels of sensitivity applicable  
44 to atmospheric radionuclide analyses [4, 5] would allow the detection of atmospheric  
45 plumes at distances of more than one thousand kilometers assuming only the oc-  
46 currence of late-time, noble gas seepage from a 5-kt UNE emplaced according to an  
47 accepted depth-to-yield relationship.

48 In this paper we evaluate the gas transport characteristics of a much lower bulk-  
49 permeability, gas containment regime. Additionally, the method for deploying the  
50 nuclear device differs from the vertical emplacement design of Barnwell. A series of  
51 access tunnels (e.g., the P-tunnel complex) was mined into the volcanic layers of Aque-  
52 duct Mesa at NNSS. Drifts were then mined into the sidewalls of the tunnels where  
53 an explosive device could be emplaced and followed by back-filling or plugging the  
54 drift with grout back to the tunnel before detonation. Among four UNEs performed  
55 in the P-tunnel complex, our research focused on the gas transport characteristics of  
56 the Disko Elm (DE) event which occurred in September 1989 having a yield less than  
57 20 kt [6].

58 At the P-tunnel DE site, we performed field experiments relevant to estimating  
59 gas leakage parameters by monitoring the propagation of atmospheric pressure fluc-  
60 tuations into the DE chimney. Additionally, we injected a Freon gas tracer into the  
61 DE chimney with the objective of determining where leakage might occur within and  
62 above the complex before escaping into the atmosphere. We found very strong evi-  
63 dence during gas sampling near surface-ground-zero (SGZ) on Aqueduct Mesa that  
64 a prolonged period of barometric low pressure, which occurred several weeks after  
65 injection, caused migration of tracer gas from the DE chimney to the surface, which  
66 our simulations suggest could be the result of soil-filled fractures with apertures so  
67 narrow as to be essentially hidden. We also detected significant leakage of tracer from  
68 the chimney and into the tunnel complex almost immediately following its injection  
69 into the chimney.

70 The field tracer injection/sampling experiments were followed by computer model-  
71 ing based on the NUFT hydrologic transport program [7]. NUFT was used to perform  
72 multi-parameter variational studies to estimate relevant leakage parameters using the  
73 atmospheric pressure data. We also used NUFT to obtain an independent evaluation  
74 of the DE chimney permeability using the Freon injection-pressure and flow rate data.

75 Using the FLEXPART atmospheric transport program [8,9], we were able to simu-  
 76 late only the possible directions of potential atmospheric signatures resulting from  
 77 the identified leaks into the tunnel complex from the chimney. The significance of  
 78 tracer detections on the surface of the mesa and in the tunnel will be considered in the  
 79 following sections. We will also include a discussion of the end-member containment  
 80 regimes we have considered to date and implications of the level of containment for  
 81 standoff detection and characterization of noble gas isotopic signatures.

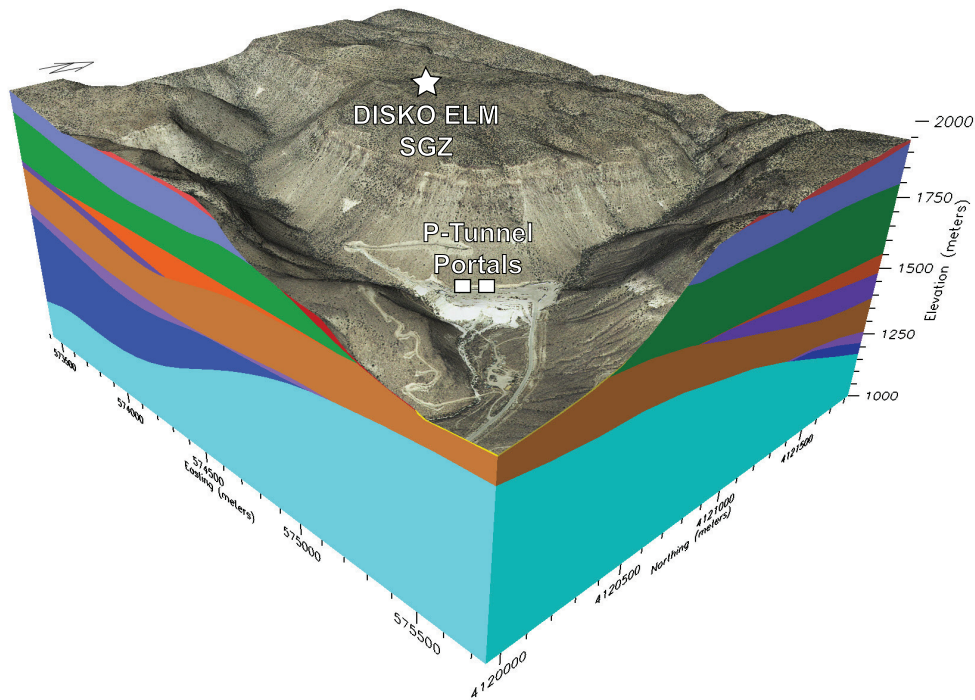


Figure 1: The Disko Elm nuclear test occurred in the P-tunnel complex within Aqueduct Mesa at the Nevada National Security Site (NNSS). The Portal at the base of the mesa accesses a tunnel at 5520 feet or 1725 m altitude. Surface-ground-zero (SGZ) or the point directly above the detonation is at 6377 feet or 1993 m altitude. The detonation point is at the tunnel level or 1725 m altitude yielding an equivalent depth of burial beneath the mesa of 268 m, which places it near the top of the UZNT or zeolitized non-welded or bedded tuff geologic formation (orange layer in figure). Image generated using EarthVision 10, Dynamic Graphics Inc., Alameda, CA. [10]

82 The device was detonated near the top of the zeolitized non-welded tuff (UZNT)  
 83 geologic unit (Fig.1, red layer) at a depth of 268 m beneath the top of Aqueduct  
 84 Mesa. Between the detonation point and SGZ there are several other volcanic for-  
 85 mations exhibiting varying levels of strength and fracture characteristics. Additional  
 86 details of the geologic cross section are provided in Fig. 2. As the post-detonation,

87 cavity-forming pressure decreased below levels capable of supporting lithostatic load-  
88 ing above the cavity, collapse of its roof occurred. The preferred model (Fig. 2) for the  
89 chimney structure resulting from the upward migration of the collapse has it extend-  
90 ing upward 141 m through two geologic units to the base of a stronger, moderately  
91 welded tuff (UWT) unit, which resisted further collapse. (Note: If the cavity reaches  
92 the surface a crater is formed, but in this case the welded layer of volcanic tuff is  
93 believed to have halted the upward migration of the void during the collapse.) This  
94 unit is also more highly fractured than the ones it overlies making it less of a barrier  
95 to gas transport from the chimney and into the surrounding zone of containment.  
96 The radius of the chimney is likely to vary with height. The angled borehole from  
97 the tunnel into the chimney intersected its boundary at a radial distance from the  
98 detonation point of 26.7 m, which we will assume to be the radius of a simplified  
99 cylindrical model of the DE chimney.

100 The interior of the zone of collapse or chimney usually consists of a zone of melt at  
101 the bottom of the chimney resulting from the heat of detonation overlain by rubblized  
102 material from the collapse of the cavity roof. The ability of the collapsed material or  
103 rubble to maintain some level of structural integrity allowing very high-permeability  
104 fracture pathways for gas to exist has usually been assumed permitting chimney  
105 models to have a uniform noble gas distribution (e.g., [2,3]). However, the low strength  
106 of the non-welded tuff in this case may allow elimination of many gas paths as a result  
107 of the crushing or compaction of the collapsed tuff during the upward cavity-migration  
108 or stopping process. For the purpose of this study, we have assumed a two-permeability  
109 cavity having a zone of lower permeability overlying a void (infinite permeability) that  
110 has migrated upward from the detonation point to the base of the moderately welded  
111 tuff unit as shown in Fig. 2.

## 112 Barometric Pressure Observations

113 LLNL has developed a gas sampling and environmental parameter logging system  
114 called the Subsurface Gas Smart Sampler (SGSS). The sampling systems are ruggedized  
115 for field use and operate indefinitely on either electrical mains power in the tunnel  
116 complex or on batteries charged by solar panels. On Aqueduct Mesa two systems ex-  
117 tracted daily soil-gas samples (0.5-liter) from beneath tarps while continuously mon-  
118 itoring barometric pressure and radon levels at SGZ. Four other SGSS units were  
119 positioned at locations in the tunnel complex to allow sampling of tunnel air after the  
120 injection of Freon tracer in addition to monitoring atmospheric pressure fluctuations  
121 in the chimney via the injection borehole and in the tunnel complex.

122 We used the barometric pressure in Non-Isothermal, Unsaturated Flow and Trans-  
123 port (NUFT) simulations [7,11] to estimate characteristic values of containment-zone  
124 bulk permeability, fracture aperture, fracture frequency and matrix permeability,  
125 which is discussed in a subsequent section. However, Fig. 3 shows several interest-  
126 ing details concerning the different pressure measurements. All the measurements,  
127 except in the cavity, overlap each other when altitude offsets are taken into account for  
128 the SGZ measurements. Even the partially sealed drift (RE-3) mined back to within  
129 approximately 6 meters of the edge of the chimney rubble zone tracks the tunnel and

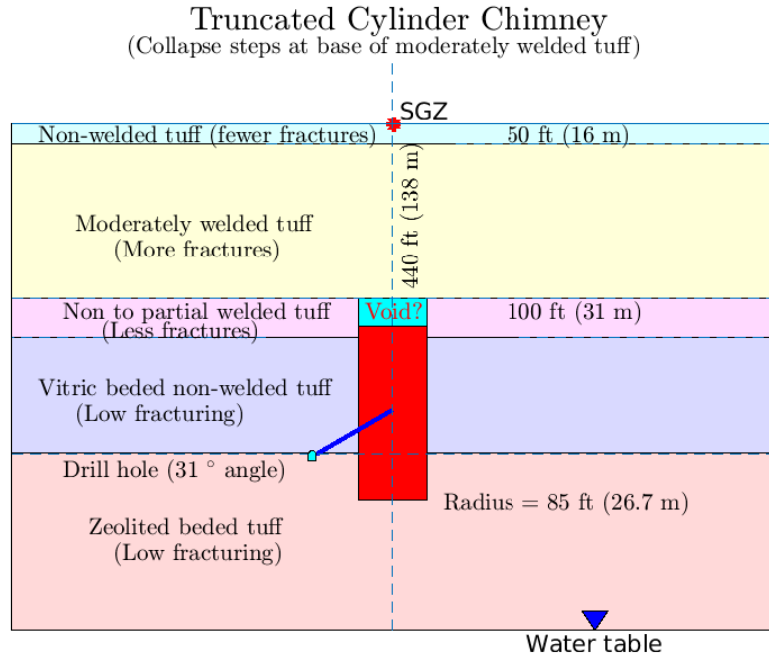


Figure 2: The relationship of the angled tracer-injection borehole to the detonation or working point is shown along with the distribution of bulk permeability assumed in this study. Both cavity injection pressure and barometric pressure are measured through this angled borehole terminating in the rubblized material resulting from the collapsed roof. This more elaborate model allows for the possibility that the lower permeability of the rubblized zone in the chimney prevents uniform mixing of tracer gas. We define characteristic bulk permeabilities for the rubble material ( $P_r$ ), the void at the top ( $P_v = \text{infinity}$ ) and the containment regime ( $P_c$ ).

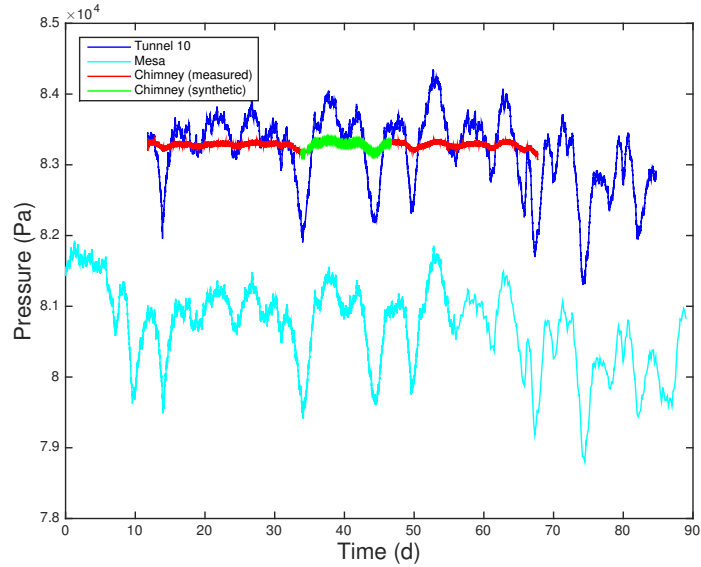


Figure 3: Illustrated are fluctuations in barometric pressure monitored in the tunnel (i.e., tunnel barometer, dark blue line) and at SGZ on the mesa surface (light blue line). The pressure offset due to the elevation difference between the tunnel and SGZ ( $\sim 268$  m) is about 25 millibars (mb). When this offset is eliminated with the different vertical scales in the figure, the pressure signals at SGZ (light blue line) and in the tunnel (dark blue) essentially overlap each other. The red line is the cavity pressure history which fluctuates very little ( $\sim 1$  mb) compared to the other measurements for most of the pressure record. For part of the record, the cavity pressure signal appears to track the tunnel pressure history because the cavity pressure-measurement line was disconnected from the borehole prior to injection to prevent damage to the pressure sensor and then left to record tunnel pressure variations. The green line is the cavity pressure synthesized using the measured atmospheric pressure fluctuations (light blue line).

130 SGZ fluctuations closely. This very good tracking of pressure fluctuations indicates  
131 that the mined-back drift is better connected to the main tunnel complex than ex-  
132 pected. Secondly, the range of cavity-pressure fluctuations is only 7–8% of the range  
133 of atmospheric fluctuations that drive the cavity-pressure changes. By comparison,  
134 the Barnwell chimney pressure variations are more than 30% of the range of atmo-  
135 spheric pressure fluctuations (Fig. 1 of [2]). The more highly attenuated amplitude  
136 of the chimney signal clearly indicates that the atmosphere-to-monitoring-borehole  
137 connection is much weaker (lower permeability) than in the Barnwell containment  
138 regime. However, is this mainly a result of the DE containment regime or the po-  
139 tentially low permeability of the zone of collapse above the monitoring borehole. We  
140 investigate this momentarily using tracer-injection-pressure monitoring data.

## 141 Freon Injection Observations

142 Prior to injection, sampling of tunnel gases was performed for several days to de-  
143 termine what gases might already be present. One of the tracer candidates, Freon  
144 13B1, was not detected in any samples. In addition to its very low to nonexistent  
145 background, the tracer is essentially inert, like a noble gas, and has a detection level  
146 of approximately 0.1 parts-per-billion-by volume (ppbv). Its molecular weight (149)  
147 is comparable to the radioxenon isotopes of interest allowing it to have a similar gas  
148 diffusivity to radioxenon.

149 During a period of almost 4 hours, we injected 63 kg of Freon 13B1 into the  
150 Disko Elm chimney along a 39 m annular region formed between two concentric tubes  
151 grouted into the borehole connecting the access tunnel to a region in the collapse  
152 zone located above the detonation or working point (Fig. 2). The Freon was co-  
153 injected with ambient air into the rubblized chimney material through the borehole  
154 for approximately 220 minutes at a rate of 200 ft<sup>3</sup> or 6.1 m<sup>3</sup> per minute. The injection  
155 rate was held constant during this period except for a very brief stoppage of the pump  
156 to determine the pressure drop, about 8 mb, along the length of the 39 m annular  
157 injection path (Fig. 3). Following this period, the flow rate was reduced to 146 ft<sup>3</sup>  
158 min<sup>-1</sup> or 4.46 m<sup>3</sup> min<sup>-1</sup> for about 20 minutes before terminating the injection. The  
159 injection-pressure history data, shown in the section of Analysis of Injection-Pressure  
160 Data, are a best fit curve since the pressure data set available to us was incomplete  
161 with a gap in the middle during the 220-minute period.

162 An important question concerning any estimate of the bulk leakage parameters of  
163 the zone of containment is how estimating these parameters by monitoring barometric-  
164 pressure-driven fluctuations might be affected when the borehole used for tracking  
165 pressure changes terminates in the rubble-filled collapsed zone. We used the injection-  
166 pressure history to estimate the role that this chimney-collapse zone of rubble plays  
167 in influencing the overall bulk leakage parameters obtained independently from the  
168 propagation of atmospheric pressure fluctuations. Two models of the distribution of  
169 gas permeability in the chimney were used to determine a best fit to the injection-  
170 pressure data, which will be considered in a subsequent section.

171 The injection was completed just before 4 pm on 18 January 2018. Gas samples  
172 were taken periodically by three smart samplers in the injection borehole access tunnel

173 as well as in the post-detonation re-entry drift via a port in the metal door to the  
174 drift and in an alcove adjacent to the re-entry drift door. The samples were then sent  
175 for analysis using a specially tuned gas chromatograph coupled to an electron-capture  
176 detector (ECD). The analyses indicated that tracer was present in the re-entry drift  
177 within 24 hours of completing the injection. Figure 4 shows how Freon levels changed  
178 with time at the three sampling locations in 1) the re-entry drift, 2) the alcove next  
179 to the re-entry drift door and 3) the access tunnel 200 m distant. It is highly likely  
180 that tracer from the Disko Elm chimney first entered the P-tunnel complex through  
181 the rear wall of the re-entry drift about 6 m from the edge of the chimney. The  
182 concentration of tracer gradually increased in the re-entry drift until it was detected  
183 beyond the drift door in the adjacent alcove and finally in the tunnel. The gradual  
184 migration of gases from the chimney into the tunnel has significant implications for  
185 the standoff detection of a tunnel-emplaced UNE especially when the containment  
186 geology may have a very low bulk permeability.

187 On the surface of the mesa at SGZ, two smart samplers were sampling periodically  
188 during a prolonged drop in atmospheric pressure of almost 22 mb over 4 days, which  
189 followed the injection by about three weeks. Between the middle and end of the  
190 period of reduced barometric pressure, gas samples taken from beneath one of the  
191 sampled tarps yielded 4 consecutive detections of Freon between 12–15 February as  
192 shown in Fig. 5. The detections of Freon terminated a period of 10 consecutive “no  
193 detects” obtained in the preceding 10-day period. It should be noted that the other  
194 smart sampler, which obtained samples every other day beneath a tarp near to the  
195 first tarp, captured no tracer during the same period. This is significant as it indicates  
196 that the source of tracer captured beneath the first tarp was highly localized, such as  
197 resulting from a fracture. Any atmospheric plume that might have originated from  
198 the tunnel portal about a kilometer distant would be expected to produce detections  
199 under both tarps at SGZ.

## 200 **Analysis of Barometric Pressure Monitoring Data**

201 We used the NUFT program to perform a best fit variational study of four leakage-  
202 related parameters to match the observed chimney borehole pressure fluctuations  
203 (Fig. 3) driven by surface barometric pressure variations. Variation of the five param-  
204 eters required for the dual permeability models (DKM) used in NUFT (bulk perme-  
205 ability, fracture aperture, fracture frequency and matrix permeability) to obtain the  
206 best fit to the borehole pressure fluctuations involved doing 1000 simulations yielding  
207 the best-fit leakage parameters in Table 1. Table 1 also characterizes the top ten best  
208 fits to provide an indication of the range of parameter variations that occurred. The  
209 smaller the range of the 5-parameter variations suggests the increasing stability of  
210 this approach to obtaining the leakage parameters.

211 The value of approximately 0.45 Darcys obtained for the bulk permeability is strik-  
212 ingly low indicating that the borehole penetrating the chimney is not well connected to  
213 the surface regarding the transport of gases to the surface especially compared to the  
214 Barnwell test site having an estimated permeability exceeding 4 Darcys [2]. How the  
215 contribution of the collapsed chimney material affects this low value of permeability

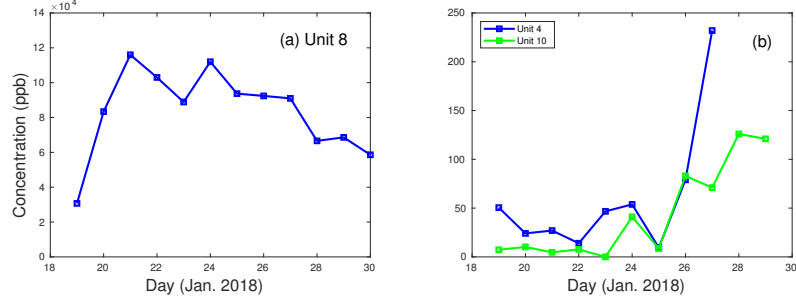


Figure 4: Freon signals versus time in the re-entry drift (a), in the access tunnel alcove outside the re-entry drift door (b, blue line) and in the access tunnel at about 200 m from the alcove by the ventilation intake (b, green line). The tracer histories indicate that the chimney apparently leaked directly into the re-entry drift producing a high concentration of tracer diluted less 1/50 of the injection concentration. Gases from the drift then diffused into the access tunnel and were transported down the tunnel to the ventilation intake where they could be potentially exhausted out the tunnel portal.

Table 1: Using a NUFT model to simulate the propagation of pressure fluctuations between the surface of Aqueduct Mesa and the monitoring borehole embedded in the Disko Elm collapse chimney, a five-parameter variation study was performed to obtain a best fit of the pressure-fluctuation history to observations. To obtain the best fit simulation yielding a bulk permeability of the containment zone of 0.45 Darcys ( $4.5 \times 10^{-13} \text{ m}^2$ ) required performing 3600 simulations. This value is about 1/10 of that obtained for the Barnwell site on Pahute Mesa. In addition to the best fits obtained for the five parameters, the maximum, minimum and means of the best 10 fits are also provided. The best-fit parameter set produced excellent agreement between the simulated and observed chimney-pressure fluctuation over the 20-day history that was considered.

Parameter	Unit	Minimum	Maximum	Mean of top 10	Best
Fracture aperture	[m]	$1.0000 \times 10^{-4}$	$1.0000 \times 10^{-2}$	$1.2442 \times 10^{-3}$	$8.4258 \times 10^{-4}$
Fracture frequency	[-]	0.5000	10.000	1.2324	1.0379
Fracture permeability	[m <sup>2</sup> ]	$1.0000 \times 10^{-14}$	$1.0000 \times 10^{-9}$	$4.9911 \times 10^{-9}$	$6.9158 \times 10^{-10}$
Matrix permeability	[m <sup>2</sup> ]	$1.0000 \times 10^{-18}$	$1.0000 \times 10^{-15}$	$9.1720 \times 10^{-18}$	$1.0014 \times 10^{-17}$
Bulk permeability	[m <sup>2</sup> ]	$2.6655 \times 10^{-18}$	$1.3801 \times 10^{-11}$	$5.1549 \times 10^{-13}$	$4.5269 \times 10^{-13}$

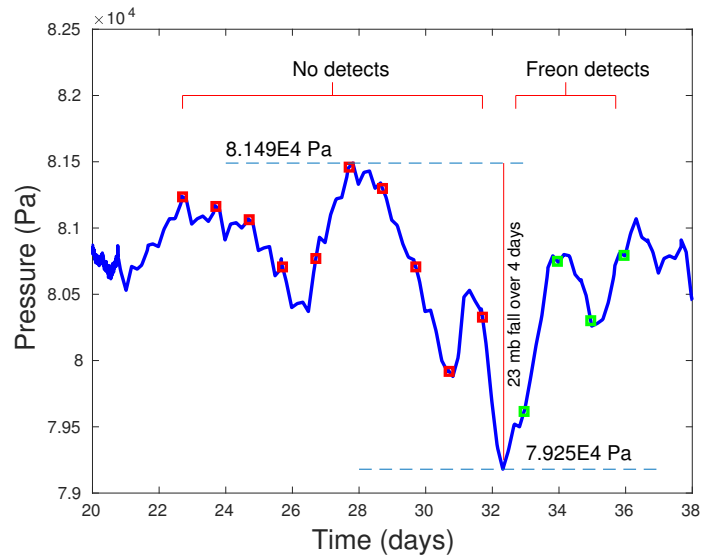


Figure 5: A long period of falling barometric pressure at SGZ coincides with the termination of 10 consecutive no detects during 2–11 February 2018 by four sequential Freon detections starting on 12 February. Barometric pressure fell 22 mb during a 4-day period. It is estimated that the altitude-corrected pressure in the chimney, which was monitored during this time, should have produced a flow toward the surface whenever the barometric pressure fell below approximately 808 mb at SGZ. All 4 detects occurred when the atmospheric pressure was either below or about 808 mb when gases would be flowing from the Disko Elm chimney. This observation further supports the fracture origin of the detections since no such requirement exists for releases to occur from the tunnel.

216 is considered in the next section.

## 217 Analysis of Injection-Pressure Data

218 Injection pressure as a function of time as measured at the tunnel-end of the injection  
219 path depends on the 1) injected flow rate, 2) resistance to turbulent flow along the  
220 injection pathway, 3) permeability of the chimney or rubble in the zone of collapse  
221 and 4) the bulk permeability of the zone of containment outside of the chimney. For  
222 a constant rate of injection, pressure increases asymptotically in time as gas flows  
223 into the surrounding chimney rubble as well as into the zone of containment beyond  
224 the chimney. If continued for a sufficiently long time, pressure will eventually reach  
225 a constant value. When this occurs, the rate of injection is entirely offset by the loss  
226 of gas into the zone of containment external to the chimney.

227 Assuming a single-permeability model for the rubble zone filling the chimney  
228 (Fig. 2), we performed a multiparameter variational analysis to obtain a best-fit  
229 match of the actual injection pressure history to the model of Fig. 2. 3600 simula-  
230 tions were performed in the process of varying containment-zone formation permeabil-  
231 ity, chimney permeability, vertical containment-zone fracture permeability, horizontal  
232 containment-zone fracture permeability and tunnel permeability where the tunnel is  
233 treated as a separate barometric pressure source. Additionally, a Sobol'-sensitivity  
234 study [12] was performed to rank order the variables by their level of impact on  
235 the pressure-history model. Table 2 lists the, best-fit values of the permeability pa-  
236 rameters, ranges assumed for each variable along with the Sobol' rank ordering of  
237 the importance of each varied parameter for obtaining the final fit. We find that  
238 containment-zone leakage properties and other parameters of Table 2 play little role  
239 compared to the bulk chimney permeability in influencing the fit of the model to the  
240 data based on the Sobol' sensitivity ranking. The best fit for the single-permeability  
241 model collapse zone is about 110 Darcys (e.g.,  $1.1 \times 10^{-10} \text{ m}^2$ ), which is a very high  
242 permeability and is presumably a result of extensive fracturing within the rubblized  
243 material in the chimney.

244 The fit of the best single-permeability material or collapse-zone model to the  
245 pressure history data in Fig. 6 is reasonable, given the level of uncertainty in chimney  
246 size and other parameters, but not ideal. The curve at early times is most poorly  
247 fit by the single-permeability model. Adding more structure to the permeability  
248 regime in the chimney was considered as a way to improve the fit. The permeability  
249 structure chosen involves two zones; a central cylindrical zone centered on the end of  
250 the borehole which is embedded in the collapse zone material. However, it was found  
251 that adding the central zone of permeability did extremely little to improve the fit  
252 between the model and observed pressure-history curves. The best fit was achieved  
253 for a central zone about 10-times more permeable than the collapse zone. In the  
254 context of the model of Fig. 2, the only really significant parameter for influencing the  
255 form of the pressure history curve is the bulk permeability of the collapse zone. The  
256 lack of perfect agreement between the two curves is not a great concern as it is clear  
257 other variables not considered, such as chimney size, shape and bulking factor (i.e.,  
258 the ratio of void volume to chimney volume) may play a role in improving the match.

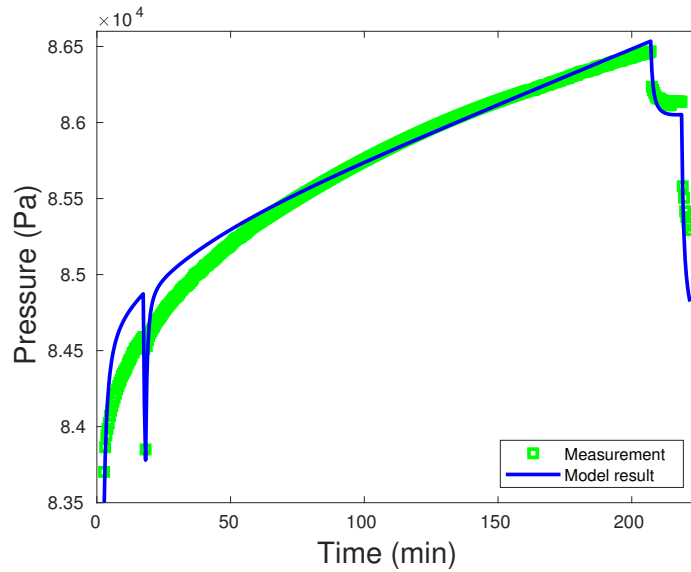


Figure 6: The green line is the pressure history for co-injection of the Freon-air mixture at an initial rate of  $6.1 \text{ m}^3 \text{ min}^{-1}$  ( $200 \text{ ft}^3 \text{ min}^{-1}$ ). After slightly more than 200 minutes or 3.6 hours, the injection flow rate was decreased to  $4.6 \text{ m}^3 \text{ min}^{-1}$  ( $146 \text{ ft}^3 \text{ min}^{-1}$ ) creating the rapid drop in pressure at the top right-side of the plot. This rate was maintained only briefly before injection was terminated at about 240 minutes or 4 hours. The match to this data for a one-permeability model representing the chimney material is given by the blue line. Both measurement and model result lines also exhibit a pressure drop out between 10–20 minutes after injection was started, which occurred when pumping was briefly halted to determine the effective pressure drop along the length of the injection pathway ( $\sim 8 \text{ mb}$ ). The agreement between measurement and single-permeability models is approximate. To improve the fit, a two-material model was considered by enclosing the end of the borehole in a cylinder with different permeability. The two-permeability model, however, did not significantly improve the fit.

Table 2: Observed and modelled injection histories were matched using a multi-parameter variational approach. The single-material model involved the 5 parameters listed above while the two-material model included a separate zone of permeability centered on the end of the borehole. Sobol' indices for the single- and double-material studies indicate that only the chimney material permeability significantly influenced the fit of matching of the model with the observations (Sobol' index is unity). The Sobol' indices and best-fit values are very similar for both single- and two-material/zone models. Only the single-material/zone values are shown here.

Permeability in	Sobol' TSI	Minimum (log <sub>10</sub> m)	Maximum (log <sub>10</sub> m)	Calibrated (m)
Matrix	$3.4766 \times 10^{-6}$	-18	-15	$1.2534 \times 10^{-16}$
Vertical fracture	$2.2988 \times 10^{-6}$	-14	-11	$1.7094 \times 10^{-13}$
Horizontal fracture	$5.7597 \times 10^{-7}$	-14	-11	$6.3941 \times 10^{-12}$
Tunnel	$2.0250 \times 10^{-6}$	-10	-8	$2.7357 \times 10^{-9}$
Chimney	1.0870	-11	-9	$1.0148 \times 10^{-10}$

259 Using a similar pressure-history matching approach, Peterson et al. (1977) [13] found  
 260 comparable order-of-magnitude estimates for the permeability of the chimney collapse  
 261 material from the Ming Blade UNE which occurred in Rainier Mesa. We achieved  
 262 our main objective in performing this analysis by obtaining an order-of-magnitude  
 263 estimate of the bulk permeability of the chimney collapse material.

264 Given the 100-Darcy estimated permeability of the chimney collapse zone, it can  
 265 be assumed that the much lower bulk permeability ( $\sim 0.45$  Darcy) determined by  
 266 propagation of barometric pressure fluctuations to the borehole monitoring point is  
 267 entirely due to the zone of containment surrounding the chimney collapse zone and  
 268 not the collapsed material itself, which is characterized by a permeability orders of  
 269 magnitude higher.

## 270 Freon Tracer Analyses

271 Based on barometric pressure observations, the tunnel complex within Aqueduct Mesa  
 272 is characterized by a bulk fracture permeability much lower than that of the high-  
 273 permeability end-member Barnwell UNE site on Pahute Mesa at the Nevada National  
 274 Security Site (NNSS). However, a low bulk permeability does not rule out the pos-  
 275 sibility that a set of sparse fractures exists over SGZ, which serve as pathways for  
 276 chimney gas transport to the surface. The apparent very high estimated permeability  
 277 of the collapse material in the chimney suggests that chimney gases may readily move  
 278 upward to the top of the chimney, which according to our preferred geologic model is  
 279 at the base of a mechanically strong, but somewhat fractured, upper partially welded  
 280 tuff (UWT) formation about 140 m below the surface (Fig. 2). Furthermore, post-  
 281 detonation damage models of UNEs support the existence of enhanced, spall-produced  
 282 fracture permeability at and just below the surface. We now consider the possibility  
 283 that the weak pressurization of the chimney during injection (averaging 15 mb) for  
 284 about 220 minutes and the subsequent barometric pumping of gases, subject to the

285 recorded barometric pressure history, can explain the observed arrivals and concen-  
286 tration levels of Freon tracer at SGZ following a long barometric low that occurred  
287 several weeks after the injection (Fig. 5).

288 Our NUFT simulations of combined injection-pressure-driven and barometric trans-  
289 port of the Freon tracer are based on the geometry of Fig. 2. The model assumes a  
290 single fracture extending from the top of the chimney to the surface over the upper-  
291 most 140 m of the containment zone. An initial Sobol' sensitivity analysis evaluated  
292 the effect of a number of model variables influencing transport along a fracture. Frac-  
293 ture aperture of the single vertical fracture and permeability of the material in the  
294 fracture were found to be the most important parameters for determining the nature  
295 of tracer transport. A two-parameter variational study was then performed for 3600  
296 combinations of these two parameters to identify the combination giving the best fit  
297 to the first arrival of Freon and also the concentrations of the tracer as measured at  
298 the same time on 4 consecutive days. As illustrated in Fig. 7, a relatively large region  
299 in the 2-D parameter space was explored involving ranges of 3 orders of magnitude for  
300 fracture permeability ( $1.0 \times 10^{-8} \sim 1.0 \times 10^{-11} \text{ m}^2$ ) and more than 2 orders of mag-  
301 nitude ( $1.0 \times 10^{-4} - 2.5 \times 10^{-2} \text{ m}$ ) for fracture aperture. The goal of this search over  
302 such large parameter ranges was to look for multiple best-fit-parameter combinations,  
303 although only one was ultimately identified falling inside the box in Fig. 7, which iden-  
304 tifies the ranges containing the five best fits to the observations. Outside the box,  
305 green-black symbols show parameter combinations falling within the top 2% of fits.  
306 It is interesting that no good match can be found unless the material in the fracture  
307 has a permeability of approximately  $600 - 700 \times 10^{-12} \text{ m}^2$  or higher. Only when the  
308 permeability of material in the fracture is around this value do good fits (top 2%)  
309 become possible and the nearly vertical distribution of the top 2% means that any  
310 fracture between 1 mm and 2.5 cm yields a comparable fit of tracer concentration  
311 history. Only when the fracture aperture falls below about 1 mm must the perme-  
312 ability of the fracture material increase further to maintain a solution in the top 2%  
313 of simulations.

314 Comparison of the simulated Freon-tracer history assuming the best-fit parameter  
315 combination (aperture =  $5.29 \times 10^{-4} \text{ m}$ , fracture material permeability =  $791 \times 10^{-12}$   
316  $\text{m}^2$ ) with the data obtained from soil-gas sampling at SGZ is shown in Fig. 8. The  
317 extremely high level of agreement between the simulation and observations was un-  
318 expected and rather remarkable considering that the model appears to match not  
319 only the time of tracer arrival at SGZ but also the concentrations of all four samples  
320 containing Freon, each obtained a day apart. We conclude that the physical model  
321 for transport by a subsurface fracture, which is subject to the observed injection and  
322 barometric pressure conditions, appears very well suited to explaining these particular  
323 observations of Freon concentrations and arrival times. That a fracture is responsible  
324 for the Freon detections obtained at SGZ is further supported by the observation  
325 that detections only occurred when atmospheric pressures at SGZ fell below cavity  
326 pressures (altitude corrected) allowing tracer to migrate toward the surface. A release  
327 from the tunnel about a kilometer distant does not have this requirement. Finally,  
328 tracer was detected beneath only one of two tarps at SGZ which is indicative of a

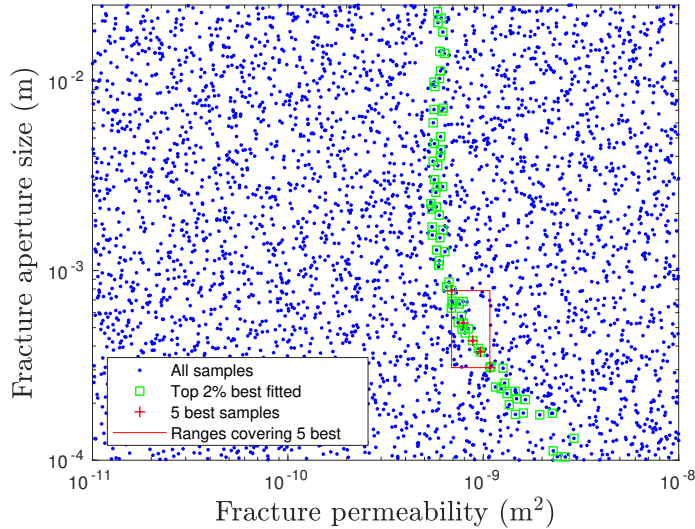


Figure 7: Fracture aperture size and fracture material permeability combinations selected in a two-parameter variational study are plotted. The study was performed to determine the single-fracture gas transport simulations with the best fits to the observed Freon arrivals and concentrations at SGZ on Aqueduct Mesa. The parameter combinations for the top 5 solutions fall within the red box giving the ranges of those parameters. The best fit is for the combination: aperture =  $5.29 \times 10^{-4}$  m, fracture material permeability =  $791 \times 10^{-12}$  m<sup>2</sup>. The green circles highlight parameter combinations that fall within the top 2% of solutions.

329 highly localized source, that is, a fracture. A non-localized atmospheric plume of gases  
 330 should be detected beneath both tarps if atmospheric infiltration had been significant  
 331 and a plume containing Freon originating from the tunnel portal was present.

## 332 Discussion and Conclusions

333 We have used barometric and gas-injection pressure histories and a gas-tracer release  
 334 to calibrate models for gas containment and release from the collapse chimney formed  
 335 by the 1989 Disko Elm UNE within the P-tunnel complex of Aqueduct Mesa at NNSS.  
 336 The results presented here contribute to understanding the nature of the source term  
 337 or types and amounts of radioactivity released to the environment following an under-  
 338 ground nuclear explosion. This has value for predicting the detectability of nuclear  
 339 explosions by on-site and standoff radionuclide monitoring systems as well as for  
 340 interpreting the characteristics of those explosions from the monitoring observations.

341 From monitoring of barometric pressure in the tunnel complex, it appears that 1)  
 342 the DE re-entry drift is well-connected to the main access tunnel, given that there  
 343 is little difference in pressure histories between the tunnel and re-entry drift. From

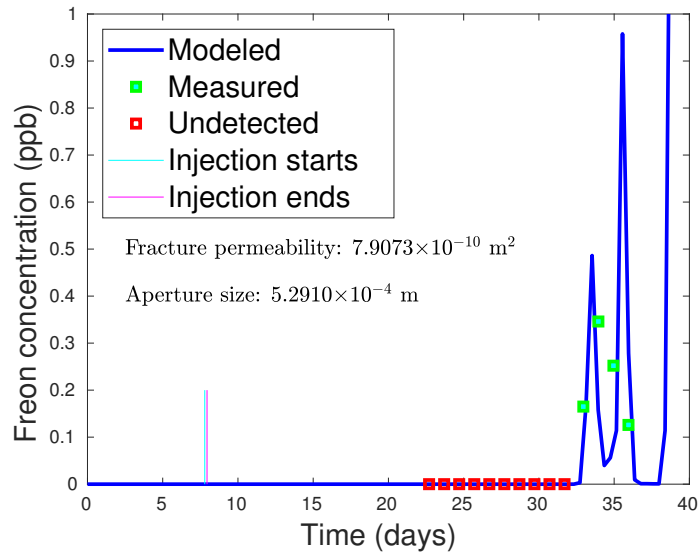


Figure 8: Comparison of the best-fit Freon tracer concentration history at SGZ with actual soil gas observations at SGZ provided by an LLNL tarp-and-sample system. The first 10 daily samples did not produce detections (open red squares), while the last 4 daily samples were detections (filled green squares). The concentration history simulation essentially matches both the first arrival of the Freon and the subsequent concentration levels measured during 4 consecutive days. Note that time (horizontal axis) is measured from the start of simulation (vertical arrow) which began about a week before the actual Freon tracer injection to initialize the simulation. The 3.6-hour Freon injection ended on 18 February 2018 (vertical mark on time axis) between 7 and 8 days after the start of the simulation. Time elapsed between Freon injection and its apparent arrival at the surface is approximately 24.3 days.

344 matching the pressure history in the DE cavity-collapse structure or chimney driven  
345 by barometric pressure fluctuations on the surface and in the tunnel, we obtained  
346 2) a bulk permeability of about  $4.5 \times 10^{-13} \text{ m}^2$  which is very much toward the low  
347 end for bulk permeabilities of UNE containment zones. The amplitude of pressure  
348 fluctuations in the cavity is only 7–8% of the fluctuations at the surface which is only  
349 a fraction of the amplitude of the fluctuation observed in the Barnwell chimney. By  
350 matching the injection-pressure history for a constant injection rate of gas into the  
351 chimney, we found that 3) the collapse zone rubble appears to have a high permeability  
352 of about  $100 \times 10^{-12} \text{ m}^2$  suggesting that injected gases should be able to flow relatively  
353 freely in the chimney during the Freon tracer injection. Further, 4) the low bulk  
354 permeability cannot be due to loss of permeability in the collapse zone but must be  
355 a result of relatively sparse fracturing in the outer containment zone.

356 Injection and monitoring of Freon 13B1 tracer provides additional information  
357 about connection of the DE chimney to both the tunnel complex and surface. We  
358 found only a day after the injection that 5) significant levels of tracer had leaked into  
359 the DE re-entry drift having an end wall only about 6 m from the estimated boundary  
360 of the chimney collapse zone. Monitoring in the adjacent access tunnel indicated that  
361 6) tracer in the sealed re-entry drift also migrated into the tunnel complex and would  
362 be eventually exhausted out the tunnel portal. Monitoring at SGZ beneath a deployed  
363 tarp yielded some surprising results 7) during a prolonged period of barometric low  
364 pressure about 3 weeks after the tracer injection when 4 detections were obtained  
365 on successive days. Fracture-transport simulations were able to provide an excellent  
366 match to the timing of the tracer arrival as well as all 4 of the measured concentrations  
367 of tracer in the samples assuming an effective fracture aperture of about 0.5 mm and  
368 a permeability of about 800 Darcys for the fracture-filling material. Such a narrow,  
369 material-filled fracture would be extremely difficult or impossible to detect by any  
370 means other than localizing the soil-gas flux using a tarp-and-sample system such as  
371 that deployed in this study. It should also be emphasized that gas transport across the  
372 subsurface is not just limited to very narrow fractures extending from the detonation  
373 point since transport can occur by fractures emanating from the top of the very high-  
374 permeability chimney, effectively shortening by about 50% the distance of transport  
375 by fractures external to the chimney.

376 While geologic considerations alone may suggest the Aqueduct Mesa test site pro-  
377 vides excellent containment of gases in the subsurface, our study supports the view  
378 that detectable gas loss via fracture transport within Aqueduct Mesa can occur follow-  
379 ing an underground nuclear explosion. The time scale of tracer arrival at the surface  
380 was appropriate for detections of most radionuclides of current interest by soil-gas  
381 sampling during on-site monitoring as well as by regional deployments of atmospheric  
382 samplers. Future tunnel studies should include both soil-gas and atmospheric sam-  
383 pling involving different released tracers to better understand relative contributions  
384 of these different modes of gas transport to the total gas released to the atmosphere  
385 from an underground nuclear explosion.

## References

- 387 [1] U.S. Department of Energy, United States Nuclear Tests, July 1945 through  
388 September 1992. National Nuclear Security Administration Nevada Field Office,  
389 DOE/NV-209-REV 16, (2016).
- 390 [2] Carrigan, C.R., Sun, Y., Hunter, S.L., Ruddle, D.G., Wagoner, J.L., Myers,  
391 K.B.L., Emer, D.F., Drellack, S.L., Chipman, V.D., Delayed signatures of un-  
392 derground nuclear explosions. *Sci. Rep.* **6**, 1–9, DOI10.1038/srep23032, (2016).
- 393 [3] Carrigan, C.R., Sun, Y., Simpson, M.D., The Characteristic release of noble  
394 gases from an underground nuclear explosion. *J. Environ. Radioact.* **196**, 91–  
395 97, (2019).
- 396 [4] Auer, M., Kumberg, T., Starorius, H., Wernsperger, B., Schlosser, C., Ten Years  
397 of development of equipment for measurement of atmospheric radioactive xenon  
398 for the verification of the CTBT. *Pure Appl. Geophys.* **167**, 471–486, (2010).
- 399 [5] Le Petit, G., Cagniant, A., Gross, P., Douysset, G., Topin, S., Fontaine, J.P.,  
400 Taffary, T., Moulin, C., Spalax<sup>RM</sup> new generation: A sensitive and selective  
401 noble gas system for nuclear explosion monitoring. *Appl. Radiat. Isotopes* **103**,  
402 102–114, (2015).
- 403 [6] Schoengold, C.R., DeMarre, M.E., Kirkwood, E.M., Radiological effluents re-  
404 leased from U.S. continental tests 1961 through 1992 DOE/NV-317. Las Vegas:  
405 Bechtel Nevada, (1996).
- 406 [7] Nitao, J.J., User’s manual for the USNT module of the NUFT code, version 2  
407 (NP-phase, NC-component, thermal). Lawrence Livermore National Laboratory,  
408 UCRL-MA-130653, (1998).
- 409 [8] Stohl, A., Forster, C., Frank, A., Seibert, P., Wotawa, G., Technical  
410 note: The Lagrangian particle dispersion model FLEXPART version 6.2. *At-  
411 mos. Chem. Phys.* **5**, 2461–2474, (2005).
- 412 [9] Stohl, A., Sodemann, H., Eckhardt, S., Frank, A., Seibert, P., Wotawa, G.,  
413 The Lagrangian particle dispersion model FLEXPART version 8.2, user manual,  
414 (2010).
- 415 [10] Dynamic Graphics, Inc., EarthVision software 10, Alameda, CA 94501, accessed  
416 August 2018, at <http://www.dgi.com>, (2018).
- 417 [11] Hao, Y., Sun, Y., Nitao, J.J., Overview of NUFT – a versatile numerical model  
418 for simulating flow and reactive transport in porous media. Edited by Zhang *et al.*  
419 in *Ground water reactive transport model*, Bentham Science Publishers, (2012).
- 420 [12] Sobol’, I., Sensitivity estimates for nonlinear mathematical models (in Russian).  
421 *Matematicheskoe Modelirovanie* **2**, 112–118, (1990).
- 422 [13] Peterson, E., Lagus, P., Lie, K., Summary of the Ming Blade tracer-gas chimney  
423 pressurization studies, DNA 4491T. Defense Nuclear Agency, Washington, D.C.,  
424 (1977).

## 425 **Acknowledgments**

426 We thank Steven A. Kreek and Kevin Grot for critical reviews, helpful discussions,  
427 and gas analyses; the National Nuclear Security Administration, Office of Defense Nu-  
428 clear Nonproliferation Research and Development (DNN R&D) and the Underground  
429 Nuclear Explosion Signatures Experiment working group, a multi-institutional and in-  
430 terdisciplinary group of scientists and engineers. We also thank the Defense Logistics  
431 Agency for their support in obtaining bottles of the Freon tracer gas and the Lawrence  
432 Livermore Professional Research and Teaching Program which provided support for  
433 revision of this paper. This research was funded by the Office of Proliferation De-  
434 tection (NA-221), U.S. Department of Energy and performed under the auspices of  
435 the U. S. Department of Energy by Lawrence Livermore National Laboratory under  
436 Contract No. DE-AC52-07NA27344 and by Mission Support and Test Services, LLC,  
437 under Contract No. DE-NA0003624.

## 438 **Author Contributions**

439 C.R.C designed experimental study and invented automated sampling system. Y.S.  
440 and M.D.S. developed models and performed simulations. S.L.H and D.G.R. designed  
441 and built auto-sampling software and hardware. C.M.O., H.E.H., L.B.P., and M.J.T.  
442 performed geological mapping and conducted field experiment.

## 443 **Additional Information**

444 **Reprints and permission** information is available at <http://npg.nature.com/reprintsandpermissions/>

445  
446 **Competing interests:** The authors declare that they have no competing interests.